

*Supporting Information for*

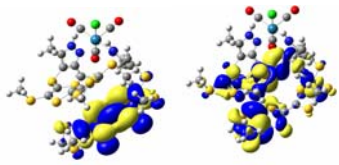
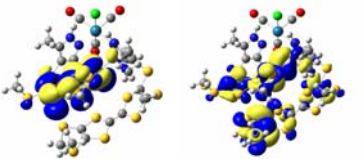
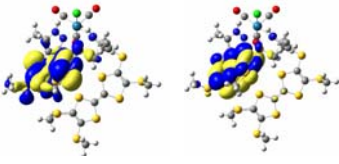
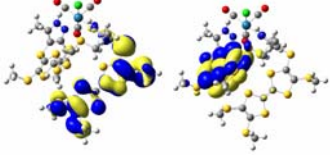
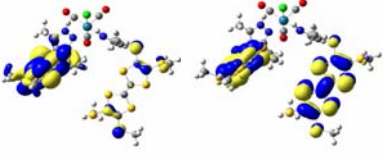
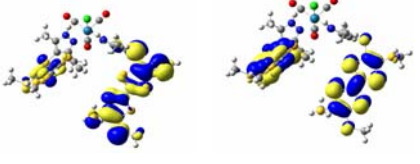
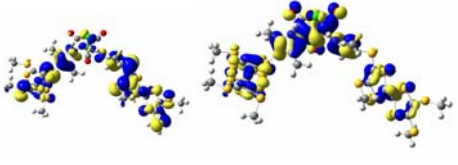
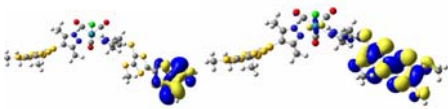
**Syntheses, Structures and Properties of Tricarbonyl (chloro)  
Rhenium(I) Complexes with Redox-Active  
Tetrathiafulvalene-Pyrazole Ligands**

Wei Liu,<sup>†</sup> Jing Xiong,<sup>†</sup> Yong Wang,<sup>‡</sup> Xin-Hui Zhou,<sup>†</sup> Ru Wang,<sup>†</sup> Jing-Lin Zuo,<sup>\*†</sup> and  
Xiao-Zeng You<sup>†</sup>

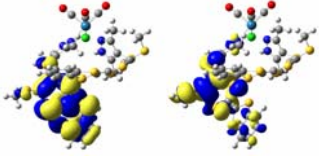
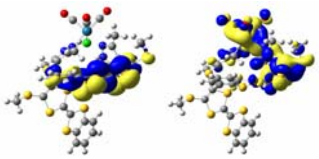
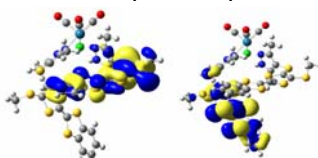
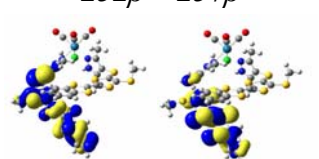
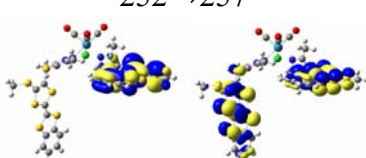
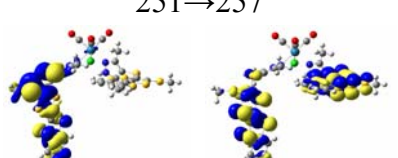
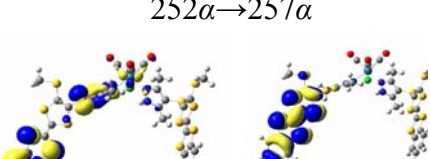
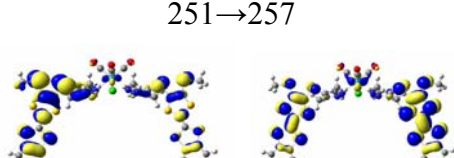
*State Key Laboratory of Coordination Chemistry, Nanjing National Laboratory of  
Microstructures, School of Chemistry and Chemical Engineering, Nanjing  
University, Nanjing 210093, P. R. China.*

*Institute of Theoretical and Computational Chemistry, School of Chemistry and  
Chemical Engineering, Nanjing University, Nanjing, 210093, P. R. China*

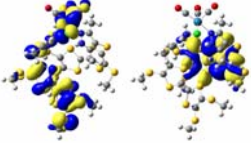
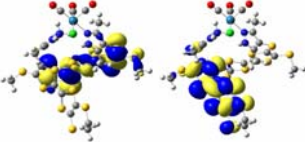
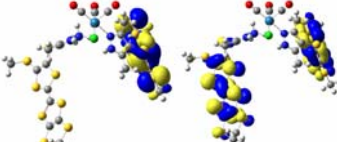
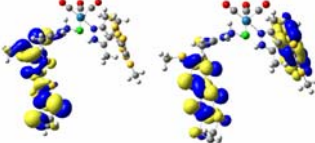
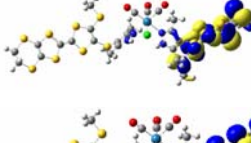
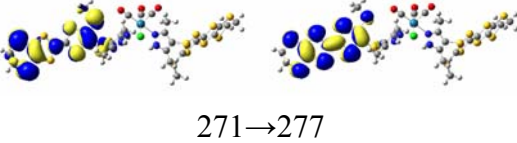
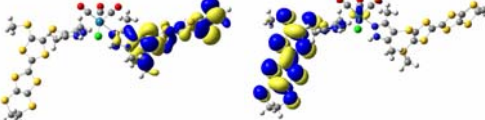
**Table S1. Main experimental and calculated optical transitions for 5a–d and their corresponding oxidized states.**

	Orbital Excitations <sup>a</sup>	Character	Calcd/nm	$f^b$	Exptl/nm
<b>5a</b>	279→283	ICT	388	0.0336	333
					
	278→282	$\pi \rightarrow \pi^*$	375	0.0426	
					
<b>5a<sup>•+</sup></b>	274 $\beta$ →279 $\beta$	$\pi \rightarrow \pi^*$	923	0.0788	823
					
	273 $\beta$ →279 $\beta$	ICT	829	0.0627	
					
<b>5a<sup>2+</sup></b>	274→279	ICT $\pi \rightarrow \pi^*$	926	0.1929	822
					
	273→279	$\pi \rightarrow \pi^*$	922	0.1160	
					
<b>5a<sup>•3+</sup></b>	270 $\alpha$ →279 $\alpha$	$\pi \rightarrow \pi^*$	1060	0.0292	822
					
<b>5a<sup>4+</sup></b>	273→278	$\pi \rightarrow \pi^*$	882	0.3561	821
					

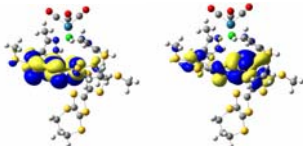
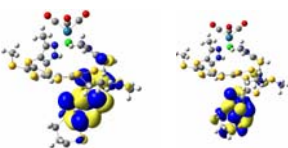
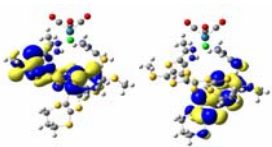
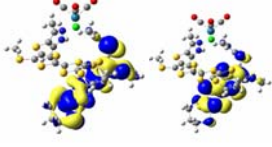
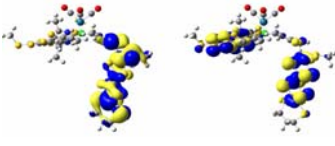
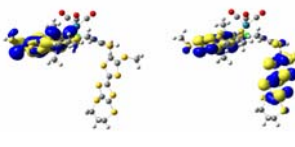
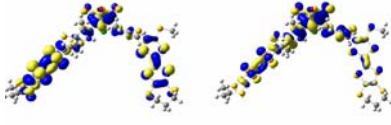
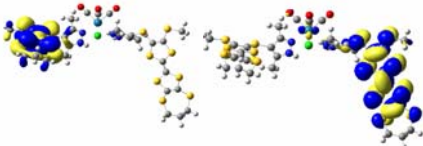
<sup>a</sup> The molecular orbital No. involved in each transition; <sup>b</sup> Oscillator strength.

	Orbital Excitations	Character	Calcd /nm	$f^b$	Exptl /nm
<b>5b</b>	256→261	$\pi \rightarrow \pi^*$	357	0.0337	358(sh)
					
	257→260	$\pi \rightarrow \pi^*$	367	0.0349	
					
<b>5b<sup>•+</sup></b>	251 $\beta$ →257 $\beta$	ICT	800	0.0986	776
					
	252 $\beta$ →257 $\beta$	$\pi \rightarrow \pi^*$	804	0.0451	
					
<b>5b<sup>2+</sup></b>	252→257	ICT $\pi \rightarrow \pi^*$	835	0.2012	768
					
	251→257	ICT $\pi \rightarrow \pi^*$	877	0.1344	
					
<b>5b<sup>•3+</sup></b>	252 $\alpha$ →257 $\alpha$	$\pi \rightarrow \pi^*$	1015	0.0124	765
					
<b>5b<sup>4+</sup></b>	251→257	$\pi \rightarrow \pi^*$	821	0.0053	777
					

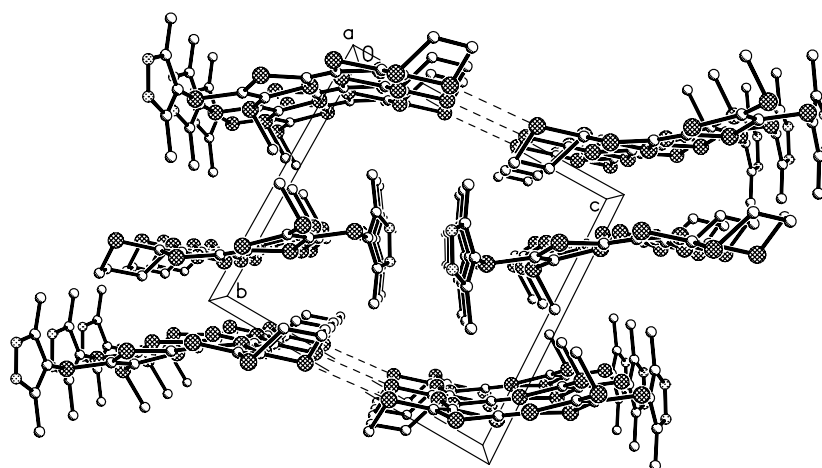
<sup>a</sup> The molecular orbital No. involved in each transition; <sup>b</sup> Oscillator strength.

	Orbital Excitations	Character	Calcd /nm	$f^b$	Exptl /nm
<b>5c</b>	276→281 	ICT	355	0.0295	343
<b>5c<sup>•+</sup></b>	271 $\beta$ →277 $\beta$ 	ICT	968	0.0842	906
<b>5c<sup>2+</sup></b>	271→277  272→277 	ICT $\pi \rightarrow \pi^*$  ICT $\pi \rightarrow \pi^*$	985  1011	0.1924	909
<b>5c<sup>•3+</sup></b>	274 $\beta$ →277 $\beta$  275 $\beta$ →276 $\beta$ 	$\pi \rightarrow \pi^*$  $\pi \rightarrow \pi^*$	937  954	0.0544	909
<b>5c<sup>4+</sup></b>	271→277 	ICT	893	0.1683	903

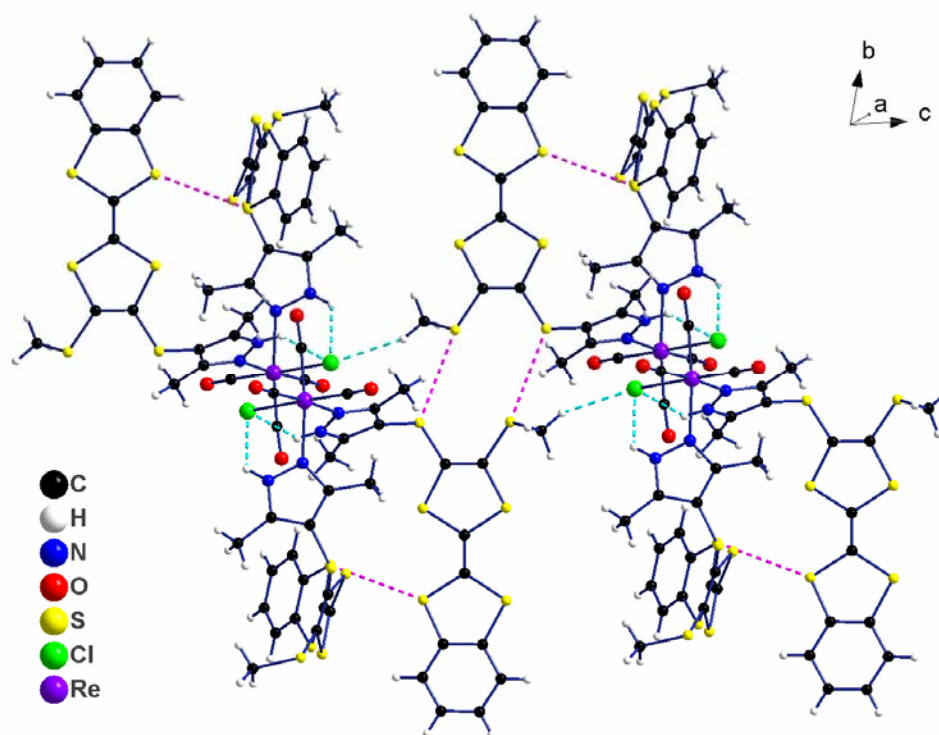
<sup>a</sup> The molecular orbital No. involved in each transition; <sup>b</sup> Oscillator strength.

	Orbital Excitations	Character	Calcd /nm	$f^b$	Exptl /nm
<b>5d</b>	285→289	$\pi \rightarrow \pi^*$	388	0.0367	337 392
					
	284→287	$\pi \rightarrow \pi^*$	392	0.0242	
					
<b>5d<sup>•+</sup></b>	279 $\beta$ →285 $\beta$	ICT	852	0.0875	815
					
	280 $\beta$ →285 $\beta$	$\pi \rightarrow \pi^*$	903	0.0587	
					
<b>5d<sup>2+</sup></b>	279→285	ICT $\pi \rightarrow \pi^*$	929	0.1303	813
					
	280→285	ICT $\pi \rightarrow \pi^*$	936	0.2113	
					
<b>5d<sup>•3+</sup></b>	283 $\beta$ →285 $\beta$	$\pi \rightarrow \pi^*$	881	0.1647	812
					
<b>5d<sup>4+</sup></b>	279→285	ICT	892	0.0015	814
					

<sup>a</sup> The molecular orbital No. involved in each transition; <sup>b</sup> Oscillator strength.

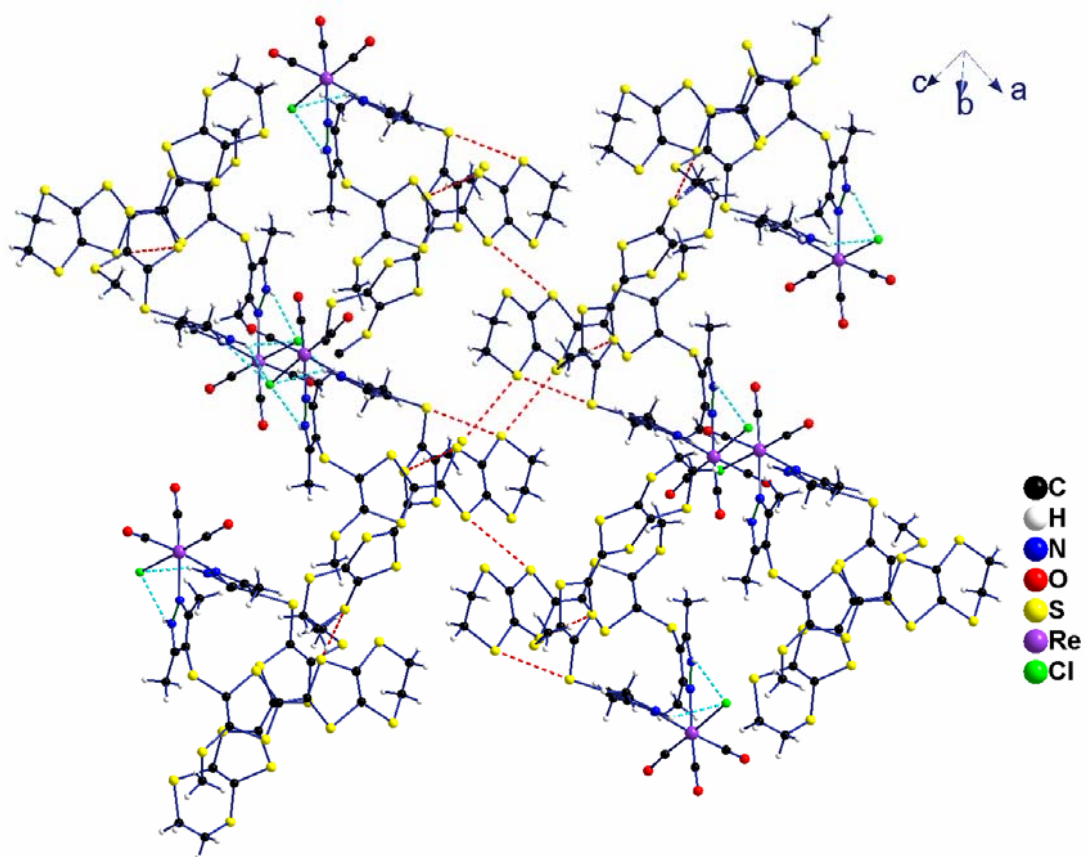


**Figure S1.** The packing diagram of compound **4d** view along the *a* axis (the dotted line representing the S...S non-bonded contacts less than 3.7 Å).

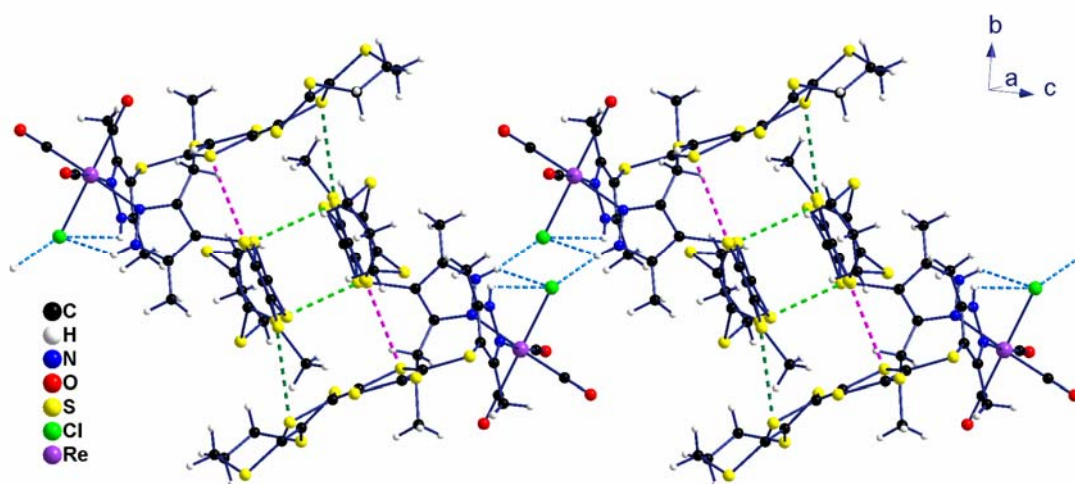


**Figure S2.** The packing diagram of compound **5b**. The dotted line representing the S...S non-bonded contacts (red) less than 3.7 Å and the H-bonding (blue).

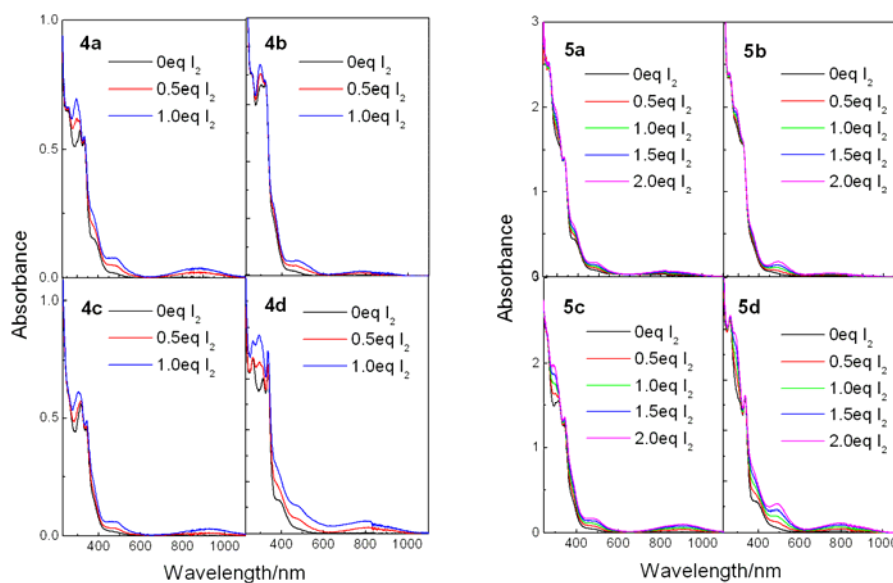




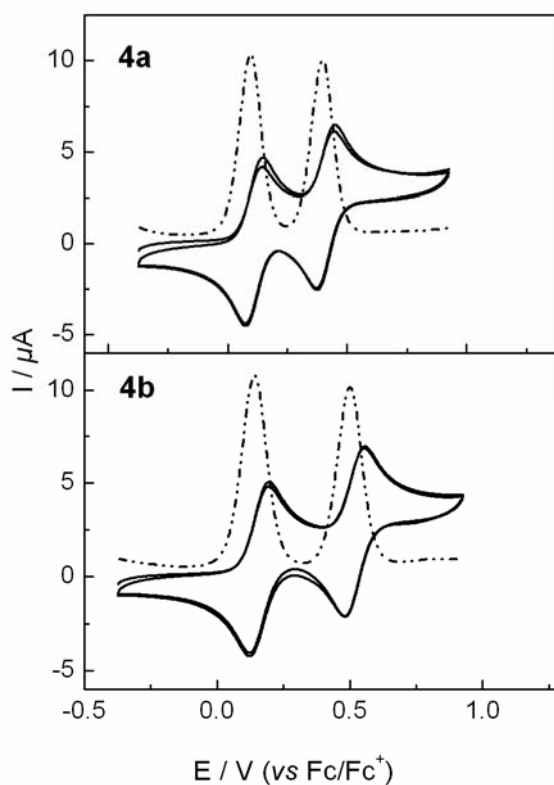
**Figure S3.** The packing diagram of compound **5c**. The dotted line representing the S...S non-bonded contacts (red) less than 3.7 Å and the H-bonding (blue).



**Figure S4.** The packing diagram of compound **5d**. The dotted line representing the S...S non-bonded contacts (red and green) less than 3.7 Å and the H-bonding (blue).

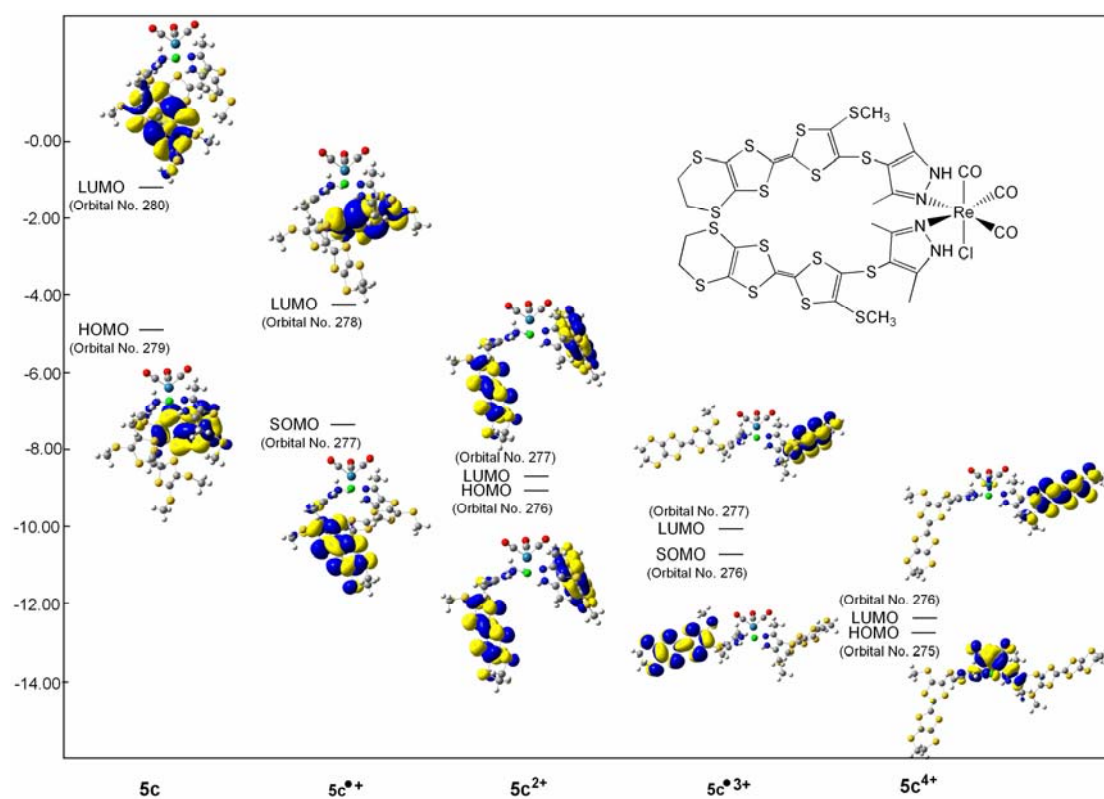
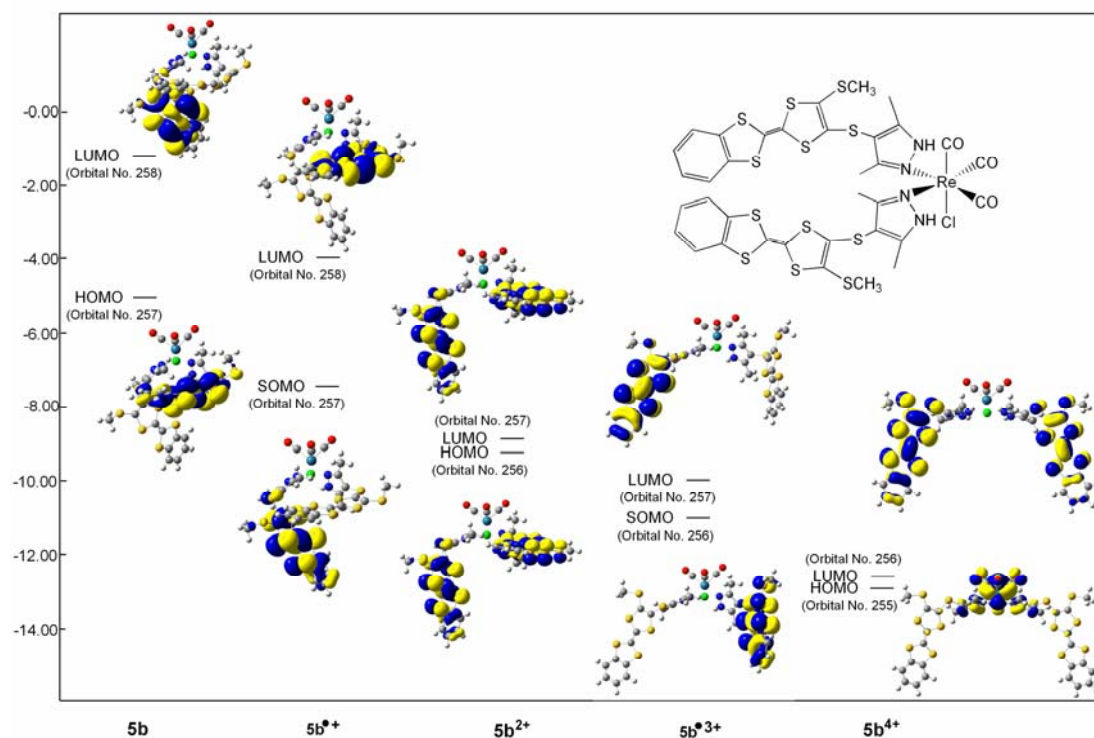


**Figure S5.** UV-vis absorption spectra for **4a–d** ( $4 \times 10^{-5}$  M) and **5a–d** ( $4 \times 10^{-5}$  M), in the presence of varying amounts of  $I_2$ , measured in  $CH_2Cl_2$ .



**Figure S6.** Cyclic voltammogram (solid line) and differential pulse voltammogram (dash-dotted line) for compounds **4a** and **4b** ( $10^{-3}$  M), measured in  $CH_2Cl_2$  (vs  $Fc/Fc^+$ ). The scan rate for CV measurements was 50 mV/s; the step increment and pulse width for DPV measurements were 4 mV and 0.05s, respectively.





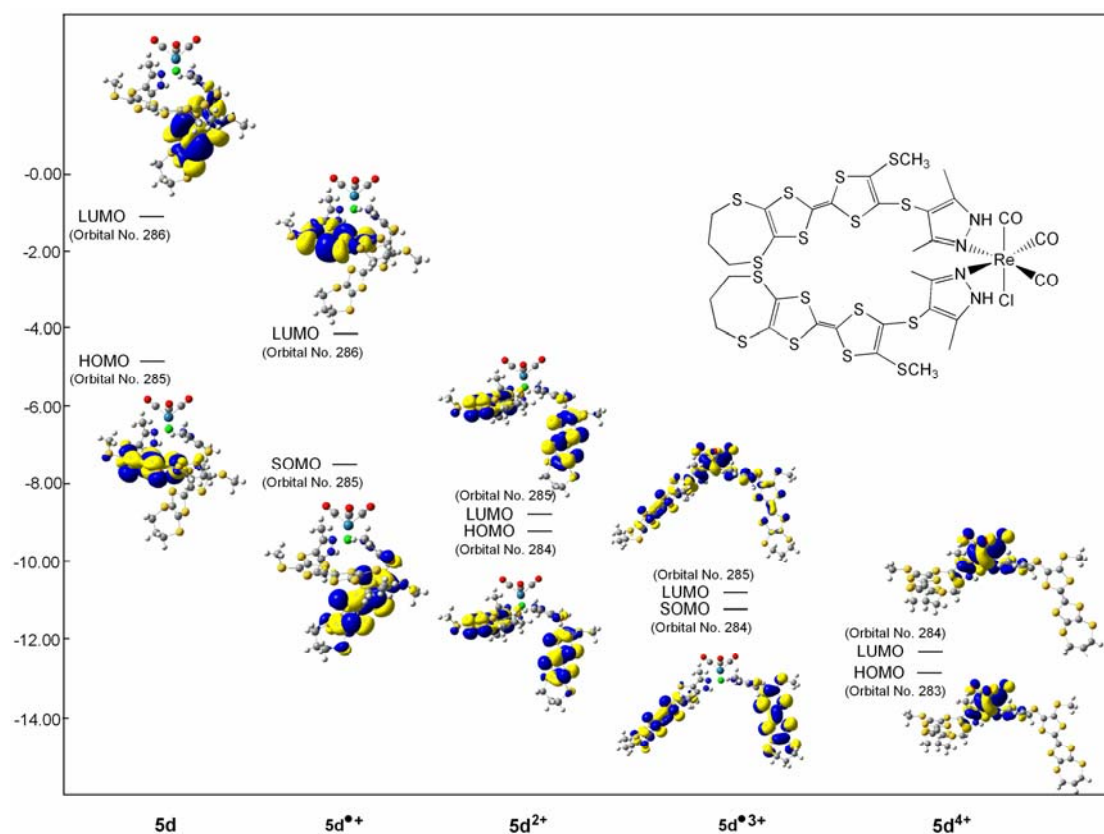


**Figure S7.** Frontier orbitals for complexes **5b–d** in the neutral, radical cation, dication, trication and tetracation states.